BIOCHEMISTRY
including biophysical chemistry & molecular biology

Article

pubs.acs.org/biochemistry

Identification of Novel Integrin Binding Partners for Calcium and Integrin Binding Protein 1 (CIB1): Structural and Thermodynamic Basis of CIB1 Promiscuity

Thomas C. Freeman, Jr.,[†] Justin L. Black,[†] Holly G. Bray,[†] Onur Dagliyan,[†] Yi I. Wu,[†] Ashutosh Tripathy,[†] Nikolay V. Dokholyan,[†,‡] Tina M. Leisner,[†] and Leslie V. Parise*[,†,‡,§]

[†]Department of Biochemistry and Biophysics, [‡]Lineberger Comprehensive Cancer Center, and [§]McAllister Heart Institute, School of Medicine, University of North Carolina at Chapel Hill, Chapel Hill, North Carolina 27599, United States

Supporting Information

ABSTRACT: The short cytoplasmic tails of the α- and β-chains of integrin adhesion receptors regulate integrin activation and cell signaling. Significantly less is known about proteins that bind to α-integrin cytoplasmic tails (CTs) as opposed to β-CTs to regulate integrins. Calcium and integrin binding protein 1 (CIB1) was previously identified as an αIIb binding partner that inhibits agonist-induced activation of the platelet-specific integrin, αIIbβ3. A sequence alignment of all α-integrin CTs revealed that key residues in the CIB1 binding site of αIIb are well-conserved, and was used to delineate a consensus binding site (I/L-x-x-x-L/M-W/Y-K-x-G-F-F). Because the CIB1 binding site of αIIb is conserved in all α-integrins and CIB1 expression is ubiquitous, we asked if CIB1 could interact with other α-integrin CTs. We predicted that multiple α-integrin CTs were capable of binding to the same hydrophobic binding pocket on CIB1 with docking models generated by all-atom replica exchange discrete molecular dynamics. After demonstrating novel *in vivo* interactions between CIB1 and other whole integrin complexes with co-immunoprecipitations, we validated the modeled predictions with solid-phase competitive binding assays, which showed that other α-integrin CTs compete with the αIIb CT for binding to CIB1 *in vitro*. Isothermal titration calorimetry measurements indicated that this binding is driven by hydrophobic interactions and depends on residues in the CIB1 consensus binding site. These new mechanistic details of CIB1−integrin binding imply that CIB1 could bind to all integrin complexes and act as a broad regulator of integrin function.

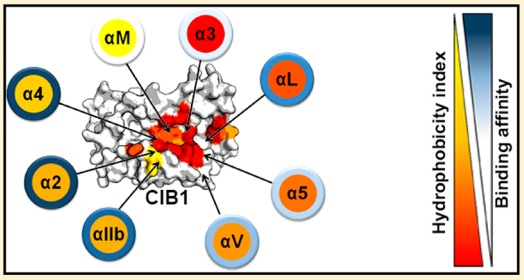

Integrins make up a large family of heterodimeric (α/β) transmembrane proteins found in almost every mammalian cell type. This family consists of 18 α-subunits and 8 β-subunits that can pair to form 24 different heterodimers. These proteins control many normal cellular processes, including migration, growth, differentiation, and proliferation.[1] Integrins also play significant roles in many diseases, including Glanzmann's thrombasthenia, various immune disorders, and cancer.[2−4] Therefore, examining the details of integrin regulation and signaling is essential.

A better understanding of the protein−protein interactions occurring at the integrin cytoplasmic tails (CTs) is necessary to elucidate the details of bidirectional integrin signaling. While there are well-understood integrin β-subunit binding proteins like talin, the kindlins, Rab25, PKCα, Src, Numb, and many others,[5,6] there are many fewer known α-subunit binding partners, e.g., Nischarin, Calreticulin, Rab21, p120RasGAP, SHARPIN, and GIPC1.[7−11] We previously reported CIB1 (calcium and integrin binding protein 1) as a binding partner for the αIIb CT of the platelet-specific αIIbβ3 integrin.[12]

CIB1 is a 22 kDa, helical, EF-hand-containing protein related to calcineurin B and is expressed in many cell types.[13−17] Previous studies revealed that highly conserved residues N-terminal to the GFFKR motif of the αIIb CT were essential for CIB1 binding.[13,18] Additionally, multiple reports indicate that CIB1 may modulate either inside-out[19] or outside-in[20,21] αIIbβ3 signaling. Besides αIIb, CIB1 binds to a variety of other proteins, including signaling proteins PAK1, Snk, and Fnk.[22,23] Although CIB1 interacts with many important signaling proteins, CIB1 knockout mice develop normally. While CIB1 is not required for normal embryonic development,[24] potentially because of compensation by CIB family members CIB2, CIB3, and/or CIB4,[25] CIB1 knockout mice exhibit phenotypic abnormalities, including impaired pathological angiogenesis, reduced levels of tumor growth, protection from cardiac hypertrophy, and male sterility.[24,26−28] Here we examined the physical relationship of the CIB1−integrin interaction to gain insight into the functional roles of CIB1.

Because CIB1 binds to a conserved region on αIIb and is ubiquitously expressed, we hypothesized that CIB1 may bind to other α-integrin CTs. We used molecular docking simulations to test the plausibility of our hypothesis and found that αIIb, α5, and αV cytoplasmic tail peptides dock to the same

Received: May 29, 2013
Revised: September 5, 2013
Published: September 6, 2013

hydrophobic binding pocket on CIB1. We show that CIB1 binds to $\alpha V\beta 3$ and $\alpha 5\beta 1$ integrins in mammalian cells via co-immunoprecipitation, demonstrating that CIB1 can interact with different whole integrin complexes *in vivo*. We also found that the CT peptides of many integrins, which included representative members of each receptor subfamily, compete with αIIb for binding to CIB1. Further, we show that binding of CIB1 to all tested α-integrin peptides is driven by hydrophobic interactions, and that there is a correlation between the hydrophobicity of the CIB1 binding site on α-integrin CT peptides and binding affinity. These findings indicate that CIB1 is an even more versatile integrin-binding protein than previously realized and suggest that CIB1 may play a common role with different integrins.

EXPERIMENTAL PROCEDURES

Protein Purification and Peptide Synthesis. Human wild-type CIB1 was cloned into pProEX HTc (Invitrogen) and further modified to include an upstream amino-terminal hexahistidine tag followed by a tobacco etch virus (TEV) cleavage site to facilitate removal of the hexahistidine tag. CIB1 mutants ^{114}IFDF/AADA, ^{152}LI/AA, and ^{173}F/A were created as previously described.[18] Mutant and wild-type (WT) CIB1 were expressed and purified from *Escherichia coli* BL21(DE3) as described previously with slight modifications as follows.[14] After the cells had been harvested, lysed by sonication, and centrifuged, the clarified cell lysate was loaded onto an AKTA Purifier UPC 100 instrument fitted with a 20 mL His-Prep FF 16/10 column (GE Healthcare). Fractions containing CIB1 were pooled and dialyzed in storage buffer [50 mM HEPES (pH 7.4), 150 mM NaCl, 10% (v/v) glycerol, and 100 μM $CaCl_2$]. The six-His tag was removed by proteolysis using His-tagged TEV, which was added at a concentration of approximately 1 mg/100 mg of CIB1 along with 1 mM DTT, and 0.5 mM EDTA. Cleavage was conducted overnight at room temperature. Mature CIB1 was isolated by subtractive Ni^{2+} affinity purification, where His-TEV was bound to the column, and CIB1 was collected in the flow-through. The DTT and EDTA were removed by dialysis in storage buffer. The protein concentration of mature CIB1 was measured by absorbance at 280 nm with an ε of 2980 cm^{-1} M^{-1}.

Peptides were synthesized by either Bio-Synthesis, Inc., or the High-Throughput Peptide Core and Arraying Facility at the University of North Carolina at Chapel Hill and purified by high-performance liquid chromatography (HPLC). Peptide masses were confirmed by matrix-assisted laser desorption ionization MS/MS on a 7400 Proteomics Analyzer (Applied Biosystems). The sequences used are listed in Table S1 of the Supporting Information.

To generate cytoplasmic tails that could be precipitated with amylose resin beads, DNA encoding either residues 1014−1039 of human WT αIIb or residues 1011−1048 of human WT αV was cloned into a pMAL vector (New England Biosystems) downstream of the *malE* gene. The fusion protein-encoding vectors were transformed into *E. coli* BL21Star(DE3) cells, which were then grown at 37 °C in 1 L of LB, and 1 mM IPTG was added to induce overexpression of the MBP−α-integrin CT fusion proteins, which continued for 4 h at 37 °C. The cultures were harvested by centrifugation, resuspended in 50 mM HEPES (pH 7.4) and 150 mM NaCl, lysed by sonication, and then clarified by centrifugation. The MBP fusion products were purified from the lysate using amylose resin beads (New England Biolabs) according to the manufacturer's instructions. Samples were dialyzed against 50 mM HEPES (pH 7.4), 150 mM NaCl, and 10% (v/v) glycerol overnight and tested for purity by SDS−PAGE, and the final protein concentration was measured using the BCA protein assay (Pierce).

All-Atom Replica Exchange Discrete Molecular Dynamics (DMD). Modeling of binding of CIB1 to α5 and αV cytoplasmic tail peptides was performed to test for potential binding interactions with CIB1, and those models were compared to a simulation of binding of αIIb to CIB1. The model of CIB1 used in the simulations was either a homology model of CIB1 based on the ligand-bound form of calcineurin B [Protein Data Bank (PDB) entry 1DGU] or the solution structure of αIIb-CT-bound CIB1 (PDB entry 2LM5).[29] The structure of αIIb was taken from PDB entry 2KNC, and α5 and αV peptide structures were modeled after the αIIb structure using I-TASSER.[30,31] The starting structure of each integrin peptide was placed approximately 40 Å from CIB1 using the edit functions of PyMol.[32] The DMD simulations were performed as described by Dagliyan et al.[33] In these simulations, the backbone atoms of CIB1 were fixed while all atoms of the peptides were free to move with some constraints added to preserve the secondary structure. The DMD engine approximates interatomic interactions by discrete square well potentials and models proteins using the united atom representation. The van der Waals forces, solvation interactions, and electrostatic interactions are modeled in a discretized manner, as well. In replica exchange, a simulation is performed in replicate at different temperatures and the structures are exchanged between the replicates at regular intervals. This robust approach allows the engine to more easily overcome energy barriers. The length of each simulation was 10^6 time units, which is approximately 50 ns of real time. After the DMD simulations had been completed, hierarchical clustering of the integrin-binding conformations, or poses representing a single instantaneous posture captured during the simulation, were performed using root-mean-square distances (rmsds) calculated over all heavy atoms in the peptide, and MedusaScore was used to evaluate the energy landscape of the clustered poses.[34] The lowest-energy complexes were taken from the largest clusters and further refined using MedusaDock to obtain the final structures.[35] Images of the models were created using PyMol. Atom pair contacts made between CIB1 and the integrin CT peptides were identified in the docking models by finding all residues on CIB1 that were within 4 Å of any side chain atom on the integrin CT peptide using PyMol.

Co-Immunoprecipitation (Co-IP). Co-IP was performed to determine whether CIB1 associates with $\alpha V\beta 3$ or $\alpha 5\beta 1$ integrin complexes in mammalian cells as previously described with some modifications.[19] HEK293T cells were maintained in DMEM supplemented with 10% FBS and 1% nonessential amino acids at 37 °C and 5% CO_2. Plasmids encoding human integrin α5 or αV were transiently transfected in HEK293T cells using Fugene (Roche) according to the manufacturer's instructions. Cells were harvested and lysed with CHAPS lysis buffer [25 mM HEPES (pH 7.4), 150 mM NaCl, 10 mM CHAPS, 30 mM NaF, 10 mM β-glycerophosphate, 0.2 mM Na_3VO_4, 1.25 mg/mL *N*-ethylmaleimide, 0.1 mM $CaCl_2$, 0.1 mM $MgCl_2$, 5% glycerol, and Protease Inhibitor Cocktail III (Calbiochem) at a 1:100 dilution]. Clarified lysates were incubated overnight with either chicken nonspecific or anti-CIB1 IgY, and immune complexes were precipitated using goat anti-chicken IgY agarose beads (Aves Laboratories, Inc.). Beads were washed three times in lysis buffer and eluted with 1×

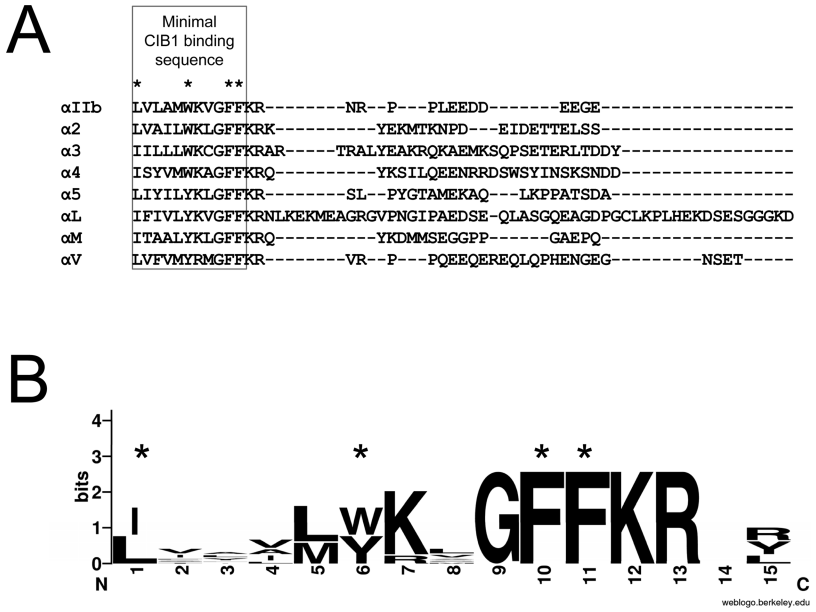

Figure 1. (A) Sequence alignment of select α-integrin tails. The minimum CIB1 binding sequence of integrin αIIb is boxed. Asterisks denote residues in αIIb that are critical for binding to CIB1. (B) Consensus logo (generated at http://weblogo.berkeley.edu/), where bits indicate the level of conservation at a position, and letter size indicates the frequency of observing a given residue at a given position.

nonreducing sample buffer. Samples were resolved by SDS−PAGE, transferred to a PDVF membrane, and immunoblotted with the rabbit anti-integrin α5 polyclonal antibody (Millipore), mouse anti-integrin αV monoclonal antibody (BD Transduction), or chicken anti-human CIB1 IgY.

Coprecipitation Assay. Purified recombinant MBP−αIIb or MBP−αV cytoplasmic tails were loaded onto amylose resin beads and washed three times in assay buffer [25 mM HEPES (pH 7.4), 150 mM NaCl, and 0.1 mM $CaCl_2$]. MBP−tail beads were added to recombinant WT or mutant CIB1 proteins diluted in assay buffer (0.75 mg/mL) and incubated for 1 h at 4 °C. Beads were washed three times with assay buffer, and samples were analyzed by SDS−PAGE.

Solid-Phase Binding Assays. Competitive inhibition solid-phase binding assays were performed to measure the binding of CIB1 to multiple α-integrin CT peptides. Various α-integrin CT peptides were immobilized in 96-well plates. Increasing concentrations of soluble peptides were used to compete with the immobilized peptide for CIB1 binding. Immulon 1B 96-well plates (Fisher Scientific) were coated with 50 μL of 50 μM peptide solutions, which were incubated overnight at room temperature (all subsequent incubations were performed at room temperature). Empty and peptide-coated wells were blocked with 3% BSA (bovine serum albumin) in PBS (phosphate-buffered saline). CIB1 (final concentrations between 0.05 and 0.1 μM) was mixed with various concentrations of the soluble peptide in 50 mM HEPES (pH 7.4), 150 mM NaCl, 0.1 mM $CaCl_2$, and 0.1 mM $MgCl_2$ and added to microtiter wells in a final volume of 50 μL/well. Solutions were discarded, and the wells were washed thrice with 200 μL of 0.05% Tween in Tris-buffered saline (pH 7.4) (TBS-T); all subsequent incubations were preceded by similar washing steps. To detect CIB1 binding, chicken anti-CIB1 IgY was added and the mixture incubated for 1 h followed by addition of HRP-conjugated donkey anti-chicken IgG (Jackson ImmunoResearch). To visualize antibody binding, a Sigma-*FAST* *o*-phenylenediamine (OPD) solution (Sigma) was added and the reaction allowed to proceed for at least 10 min. The reaction was terminated by addition of 4 N H_2SO_4, and the absorbance was measured at 490 nm in a 96-well microplate reader (Spectramax M5).

Isothermal Titration Calorimetry (ITC). ITC was performed to quantify the thermodynamics of binding between CIB1 and α-integrin tail peptides as previously described with minor modifications.[13] Purified CIB1 was dialyzed extensively in 50 mM HEPES (pH 7.4), 150 mM NaCl, and 0.1 mM $CaCl_2$ (unless noted differently elsewhere) and diluted to a concentration of 100 μM. Peptides were freshly dissolved to concentrations ranging from 0.8 to 1 mM in the same buffer as CIB1. Isothermal titrations were performed using a MicroCal VP-ITC microcalorimeter. Injections of 10 μL of peptide were added at 300 s intervals at either 15 or 26 °C. The heats of dilution were estimated from injections made after saturation had occurred. These values were subtracted from the data before one-site curve fitting was performed using Microcal, LLD Origin 7. The stoichiometry (N), association and dissociation constants (K_a and K_d, respectively), and enthalpy change (ΔH) were obtained directly from the data, and the Gibbs free energy change (ΔG) and entropy change (ΔS) were calculated with eqs 1−3.

$$\Delta G = \Delta H - T\Delta S \quad (1)$$

$$\Delta G = -RT \ln K_a \quad (2)$$

$$K_d = 1/K_a \quad (3)$$

RESULTS

Sequence Conservation of α-Integrin CTs. The C-terminal sequences of several α-integrin subunits were aligned to assess the likelihood that CIB1 could bind to other integrins besides αIIb. The alignment in Figure 1 shows several highly conserved residues in the membrane-proximal region of the integrin tails, revealing an I/L-x-x-x-L/M-W/Y-K-x-G-F-F consensus motif. The consensus sequence is conserved in all 18 α-integrin CTs (Figure S1 of the Supporting Information).

dx.doi.org/10.1021/bi400678y | *Biochemistry* 2013, 52, 7082−7090

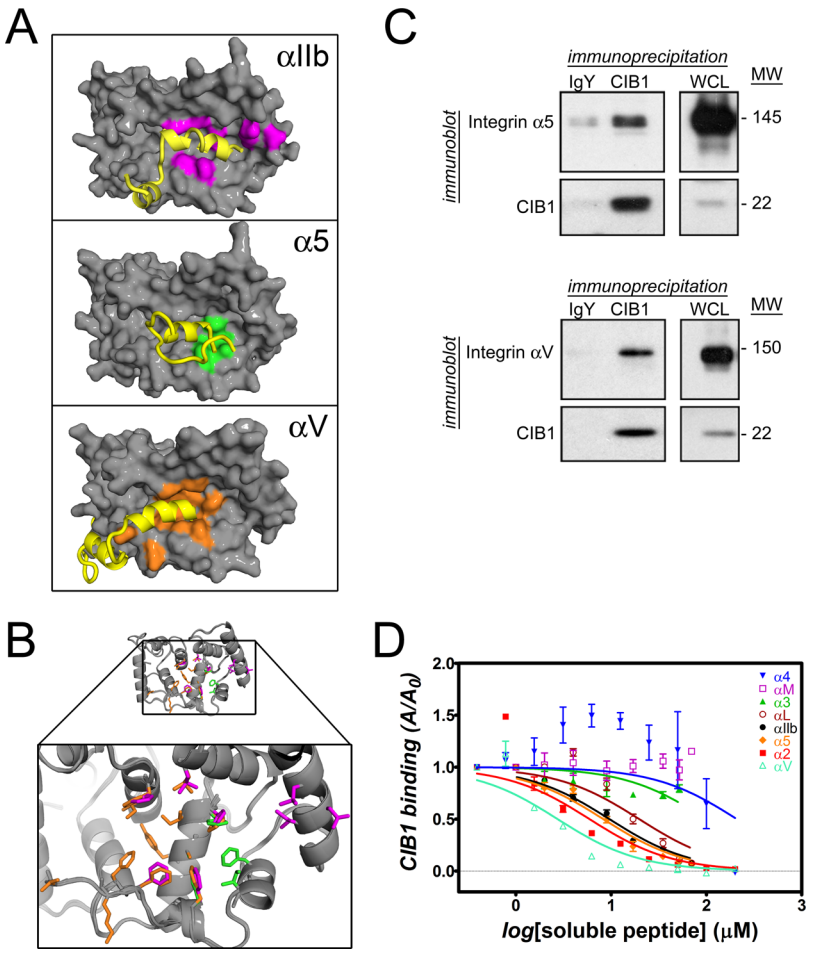

Figure 2. α-Integrin binding site of CIB1. (A) Lowest-energy structures of molecular docking of α-integrin peptides (yellow cartoons) to CIB1 (gray surface). The integrin peptide is indicated in each panel. Residues close enough to contact each peptide are colored on the CIB1 surface model. (B) Overlay and close-up of integrin binding residues on CIB1 determined from docking with αIIb (magenta sticks), α5 (green sticks), and αV (orange sticks). (C) Immunoprecipitates and whole cell lysates (WCL) from HEK293T cells overexpressing either integrin α5 or αV were lysed and immunoprecipitated with either control IgY or anti-CIB1 IgY and immunoblotted with anti-integrin α5 (top) or anti-integrin αV (bottom), while CIB1 was detected by immunoblotting with an anti-CIB1 antibody. Irrelevant lanes between the immunoprecipitate and WCL lanes were excluded by cropping the images. (D) Competitive inhibition binding assays were used to test the binding of CIB1 to eight α-integrin tail peptides. CIB1 binding (y-axis), as measured by the absorbance of OPD (o-phenylenediamine) at 490 nm and normalized to A_{490} at the lowest peptide concentration (A_0), is compared to increasing concentrations of a given solution-phase α-integrin peptide (x-axis). Data points represent means ± the standard error of the mean (N = 2) and were fit with a dose−response curve.

This observation led us to hypothesize that CIB1 can bind to most other integrins and potentially contribute to their signaling pathways. Each α-integrin CT shown in Figure 1 was tested for binding to CIB1. We selected a functionally diverse subset of α-integrins that included αV, the only other β3 integrin partner, the ubiquitous fibronectin receptor, α5, which binds to the R-G-D sequence, and some commonly observed representatives from other receptor subclasses: a laminin receptor (α3), a collagen receptor (α2), leukocyte-specific receptors (αM and αL), and a non-RGD fibronectin receptor (α4).[1]

Docking of α-Integrin CTs to CIB1. We attempted to identify the most likely integrin binding site on CIB1 using replica exchange discrete molecular dynamics (DMD) simulations (Figure 2A). The starting CIB1 structure, a homology model of calcineurin B (PDB entry 1DGU), was chosen because it has the C-terminal helix of CIB1 displaced, which is a key mechanism in integrin binding by CIB1.[36,37] This model of CIB1 was sufficient for the purposes of qualitatively assessing the likelihood of CIB1 interacting with multiple integrins. Representatives of the most frequently sampled conformations from the lowest-energy clusters of these simulations indicate a significant overlap in the binding sites occupied on CIB1 by each α-integrin CT tested (Figure 2B). Furthermore, the integrin residues that were close enough to contact CIB1 included at least the first three N-terminal hydrophobic residues of each integrin peptide. The GFFKR motifs were involved in the binding interfaces of only αIIb and αV, with both Phe^{1023} and Phe^{1024} in αIIb contacting CIB1 and only Phe^{1020} of αV making contact. As a consequence of the sequence variation of the α-integrin CTs and the randomized sampling of the simulation, the number of atom pair contacts formed between CIB1 and each α-integrin CT varied; αIIb, α5, and αV appeared to contact 9, 5, and 12 residues on CIB1, respectively.

Association of CIB1 with αVβ3 and α5β1 Integrins in Mammalian Cells. Because we predicted that CIB1 could bind to α5 and αV integrins in simulations, we asked if we could detect binding of CIB1 to integrins in cells via co-immunoprecipitation assays. Endogenous CIB1 was immuno-

dx.doi.org/10.1021/bi400678y | Biochemistry 2013, 52, 7082−7090

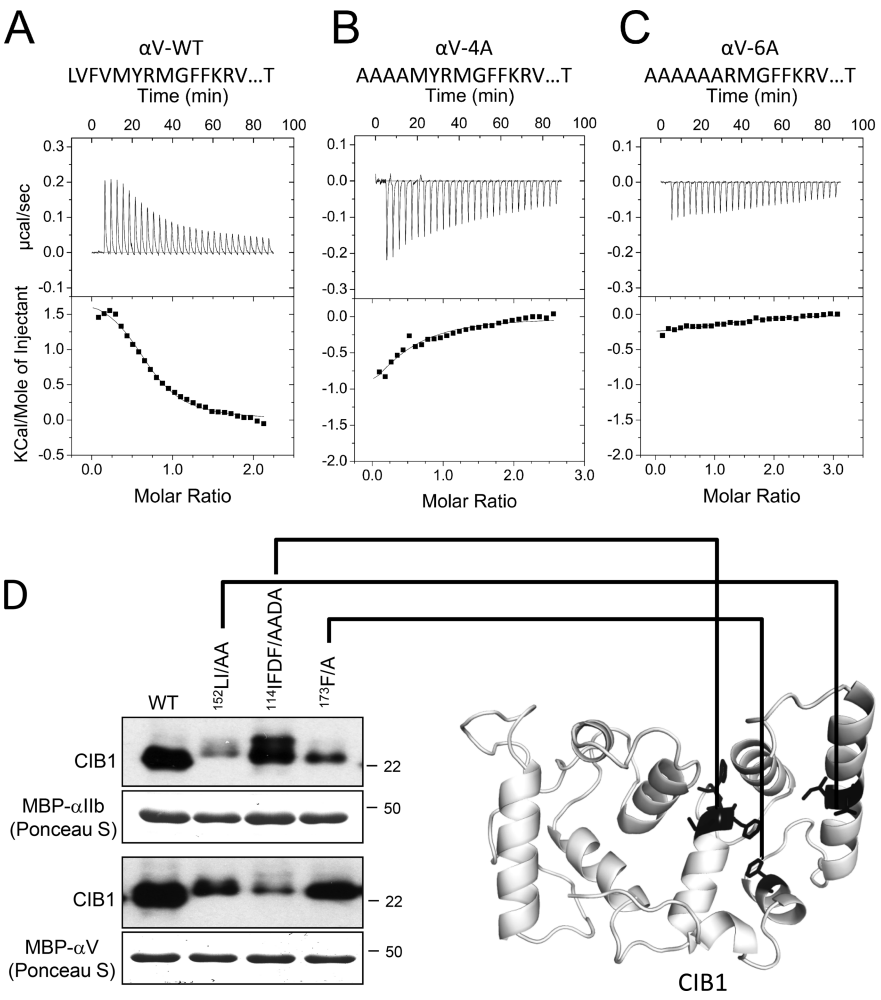

Figure 3. Validation of interaction sites predicted by DMD. Isotherms (top) and integrated peaks fit with the one-site binding model (bottom) of (A) αV-WT, (B) αV-4A, and (C) αV-6A. Data of αV-4A and αV-6A do not reasonably fit any standard binding models. (D) CIB1 coprecipitation with MBP−αIIb CT and MBP−αV CT fusion proteins. Various CIB1 mutants, indicated above the lanes and highlighted (black) on the structure to the right, were tested for their ability to bind to α-integrin CTs.

precipitated from HEK293T cells overexpressing either integrin α5 or integrin αV (Figure 2C), and both integrins coprecipitated with CIB1.

Competitive Binding of α-Integrin CT Peptides to the αIIb Binding Site of CIB1. Because molecular docking suggests that α5 and αV peptides can bind to sites overlapping that of αIIb, we tested the ability of various α-integrin CTs (see Table S1 of the Supporting Information) to compete with the αIIb CT peptide for CIB1 binding in competitive solid-phase binding assays. Most solution-phase integrin peptides dose-dependently inhibited binding of CIB1 to the αIIb CT peptide (Figure 2D). The IC_{50} ± 95% confidence interval values of αIIb, α2, α5, αL, and αV were 9.6 ± 1.1, 6.0 ± 4.0, 8.3 ± 1.3, 19.7 ± 6.7, and 2.7 ± 1.3 μM, respectively. The relatively weak competitive inhibition of CIB1 binding by αM, α3, and α4 CT peptides was not sufficient to determine IC_{50} values.

Effect of Integrin N-Terminal CT Residues on CIB1 Binding. Previous data show that the hydrophobic N-terminal residues on the αIIb CT peptide are important for binding to CIB1.[18] We therefore asked if changing residues in this region of αV would similarly disrupt binding to CIB1. Binding of CIB1 to αV peptides with either four or six alanine substitutions at the N-terminus (αV-4A or αV-6A, respectively) was compared to binding of CIB1 to αV-WT via ITC (Figure 3A−C). While αV-WT binds to CIB1 endothermically with a 1:1 stoichiometry and a K_d of 4.3 μM, isothermal data for αV-4A and αV-6A appear to have been generated primarily from heats of dilution of the peptides, and we could not reliably fit these data to any standard binding models. Thus, modifying the N-terminal residues of the αV CT significantly weakened binding to CIB1.

Effect of Mutating Residues in the CIB1 Hydrophobic Pocket on Integrin Binding. We used previously generated CIB1 mutants shown to inhibit binding to αIIb to determine if these mutations could also inhibit binding to different integrins.[18] These mutated residues are also a part of the hydrophobic binding surface on CIB1 and formed atom pair contacts with the integrin peptides in the docking simulations. We tested binding of CIB1 mutants ^{152}LI/AA, ^{114}IFDF/AADA, and ^{173}F/A to MBP−αIIb CT and MBP−αV CT fusion proteins (Figure 3D). The Western blots show that all tested CIB1 mutations differentially affect binding to distinct integrins. Notably, CIB1 ^{152}LI/AA and ^{173}F/A mutations significantly weakened binding of CIB1 to the αIIb CT fusion protein, whereas the ^{114}IFDF/AADA mutation significantly weakened binding to the αV CT fusion protein.

Role of Hydrophobic Interactions in Binding of CIB1 to α-Integrins. To further characterize the mechanism of binding between CIB1 and α-integrin CTs, we used isothermal

dx.doi.org/10.1021/bi400678y | Biochemistry 2013, 52, 7082−7090

Table 1. ITC of CIB1 and α-Integrin Cytoplasmic Tail Peptides[a]

integrin	N	K_d (μM)	ΔH (kJ/mol)	$T\Delta S$ (kJ/mol)	ΔG (kJ/mol)
αIIb	0.9 ± 0.0	1.4 ± 0.1	−16.4 ± 0.1	17.1	−33.4
αIIb[b]	1.2 ± 0.0	3.1 ± 1.8	−34.1 ± 2.2	−2.4	−31.7
α2	1.1 ± 0.0	0.9 ± 0.3	5.0 ± 0.2	39.7	−34.6
α3	1.0 ± 0.0	5.1 ± 1.0	4.2 ± 0.1	34.6	−30.4
α4[b]	0.8 ± 0.0	0.4 ± 0.1	32.7 ± 0.5	67.9	−35.2
α5	0.9 ± 0.0	6.9 ± 0.4	21.4 ± 0.3	50.7	−29.3
αL	1.1 ± 0.0	3.2 ± 0.6	8.2 ± 0.4	39.5	−31.3
αM	1.1 ± 0.0	23.6 ± 1.4	8.8 ± 0.2	35.2	−26.4
αV	0.9 ± 0.0	4.3 ± 0.9	7.3 ± 0.4	38.0	−30.7
αV-4A[c]	ND	>100 μM	ND	ND	ND
αV-6A[c]	ND	≫100 μM	ND	ND	ND

[a]Representative titration isotherms are shown in Figure S2 of the Supporting Information. Errors are from fitting the ITC data to a one-site model. Errors are not shown for $T\Delta S$ or ΔG as those are calculated values. [b]ITC of α4 was performed in ITC buffer without any NaCl because of peptide solubility issues. Binding of αIIb to CIB1 was also tested in the absence of NaCl with insignificant effects on the binding affinity. However, the thermodynamic properties suggest a change in the mechanism of binding. [c]ND, not determinable. The CIB1 binding affinities of these ligands must be greater than the upper limit of detection for ITC (100 μM).

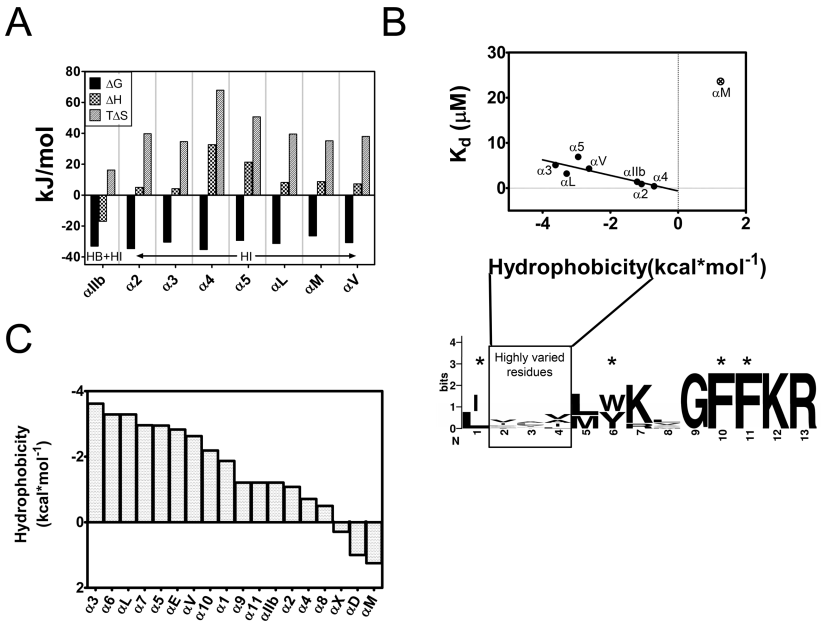

Figure 4. CIB1 binds to α-integrin CTs through hydrophobic interactions. (A) Thermodynamic profiles of binding of CIB1 to α-integrins. Free energy ΔG (black), enthalpy ΔH (checkered), and entropy $T\Delta S$ (gray) are plotted for binding of CIB1 to the α-integrin CTs shown on the x-axis. The thermodynamic profiles indicate which types of interactions, HB (hydrogen bonding) or HI (hydrophobic interactions), drive binding. (B) N-terminal hydrophobicity of α-integrin CT peptides correlates to CIB1 binding affinity. The CIB1 binding affinity of each α-integrin CT as determined by ITC (y-axis) is compared to the total hydrophobicity of the region indicated in the consensus logo below the plot (residues 2−4) of each peptide (●). Data were fit with a linear regression model (R^2 = 0.72). The value of αM (⊗) was excluded from the regression as an outlier using the ROUT method of Graphpad Prism 5 with threshold Q = 1.0%. (C) Hydrophobicity of residues 2−4 of each α-integrin CT peptide ranked in order of most hydrophobic to least.

titration calorimetry (ITC) to measure the binding thermodynamics between CIB1 and additional α-integrin CT peptides. The binding data show a stoichiometry of 1:1 with micromolar binding affinities between CIB1 and all α-integrin peptides tested (Table 1 and Figure S2 of the Supporting Information), which is consistent with previously measured binding affinities between CIB1 and αIIb.[13,38−40] In contrast to the competitive ELISA results where neither α3 nor αM competed effectively with immobilized αIIb for CIB1 binding (Figure 2D), ITC results indicated that the α3 and αM CT peptides do bind CIB1, albeit with affinities significantly lower than that of αIIb. While the binding affinities of the weakest CIB1-binding peptide and the strongest vary by an order of magnitude, the thermodynamic characteristics are similar. With the exception of the exothermic binding exhibited by binding of CIB1 to the αIIb CT peptide, binding of CIB1 to all other peptides was endothermic. The thermodynamic profiles of binding of CIB1 to the various α-integrin CT peptides suggest that the CIB1−integrin interaction is mainly driven by hydrophobic interactions (Figure 4A).[41] Overall, CIB1 bound to α-integrin CTs with a similar stoichiometry, affinity, free energy, and entropy.

Correlation between the Hydrophobicity of N-Terminal CT Amino Acids and CIB1−Integrin Binding Affinity. We reexamined the α-integrin peptide sequences to identify potential factors that may explain why there was some

dx.doi.org/10.1021/bi400678y | Biochemistry 2013, 52, 7082−7090

variance in CIB1 binding thermodynamics, and determined that the most sequence variance within the CIB1 binding region occurred among the N-terminal residues (Figure 4B). Given the potential variability in CIB1−integrin atom pair contacts and an apparently dominant role played by hydrophobic interactions in CIB1−integrin binding, we asked if there was a relationship between the hydrophobicity of the N-terminal membrane proximal region of the integrins and CIB1 binding affinity. We used the empirically defined Wimley−White water−octanol scale (where more negative values indicate greater hydrophobicity) to calculate the total side chain hydrophobicity of the highly varied membrane-proximal residues (residues 2−4) of each α-integrin CT peptide tested.[42] Linear regression of the data reveals a negative correlation between the total hydrophobicity of the highly varied region of the α-integrin peptides and the CIB1 binding affinity measured by ITC, with a slope of −1.7 ± 0.5 and an R^2 of 0.72 (Figure 4B). The calculated hydrophobicities in the highly varied region of all α-integrin CTs are within the range (−3.62 to 1.25 kcal/mol) of the tested set of α-integrin CTs (Figure 4C).

DISCUSSION

Because integrin function is regulated by cytoplasmic tail-binding proteins and the potential regulatory roles played by α-integrin binding proteins have been less studied than those played by β-integrin binding proteins, we explored the α-integrin binding capabilities of CIB1. CIB1 is ubiquitously expressed and interacts with a region of the platelet-specific integrin αIIb cytoplasmic tail that is well-conserved in all α-integrins. These observations suggested that CIB1 can bind to other α-integrins.

To efficiently assess the feasibility of testing the hypothesis that CIB1 binds to other α-integrin CTs, we used discrete molecular dynamics (DMD) simulations, which have been successfully employed in various capacities to obtain accurate estimates of protein−peptide interactions using only structural data of the receptor and ligand as input.[33,43] The docking simulations showed structural details of binding of CIB1 to αIIb, α5, and αV CT peptides, and a comparison to the recent CIB1−αIIb complex structure[15] validated that these simulations produced plausible models. The interaction interface predicted by the docking simulations was supported by mutational analysis in which CIB1 mutants in the hydrophobic binding surface selectively affected binding to different integrins, and Ala substitutions in integrin peptides disrupted binding to CIB1. The positive results from the simulations suggested not only that CIB1 can bind to multiple α-integrins but also that multiple integrins bind to the expected hydrophobic surface on CIB1. This result led us to test whether CIB1 could actually bind to multiple integrins in cells. We therefore co-immunoprecipitated whole integrins; the results validated that CIB1 can bind to other integrins in cells, as it does αIIbβ3.[13] Furthermore, competitive binding experiments showed that several α-integrin CT peptides compete with the αIIb CT for CIB1 binding, which supported the simulation data that showed that integrins bind to the same general region on CIB1. Interestingly, integrins α3, αM, and α4, which have sequences least similar to that of αIIb, competed poorly with αIIb for CIB1 binding. As expected, ITC measurements showed that the binding affinity of αM may not be strong enough to compete with αIIb under the tested conditions. In contrast, the CIB1 binding affinities for α3 and α4 are likely strong enough to compete with αIIb, if competition is for the same binding site. This supports a possibility raised by docking simulations that different integrins may bind to different local binding sites within the same pocket on CIB1. Further, the possibility of integrins binding to different binding sites within the hydrophobic binding pocket of CIB1 was supported by *in vitro* coprecipitation assays using various CIB1 mutants and MBP−integrin CT fusion proteins. Three different sets of CIB1 mutations differentially affected binding of CIB1 to two different α-integrins, suggesting that while integrins may bind within the same binding pocket, the specific molecular contacts are different. Furthermore, mutations in CIB1 around the Mg^{2+} and Ca^{2+} binding site in EF-hand III that were previously shown not to affect αIIb binding[44] did affect αV binding. This localized specificity may explain how CIB1 is able to bind to many different individual integrins using the same binding pocket. This dynamic binding capacity of CIB1 may also be heavily influenced *in vivo* by Mg^{2+} and Ca^{2+} concentrations, which have dramatic effects on CIB1 structure and binding affinity.[16,36,37,40,44]

In addition to identifying the integrin-binding site on CIB1, we also validated that the highly conserved membrane-proximal region of α-integrin CTs is the CIB1 binding site. Substituting alanine residues for a series of N-terminal residues in the αV CT peptide abolished binding to CIB1, which is in agreement with previous reports that these residues are important for binding of CIB1 to αIIb.[18] We can therefore infer that these hydrophobic residues in the consensus binding sequence are essential for binding of CIB1 to all α-integrin CTs. Moreover, we have shown that there is a correlation between the total side chain hydrophobicity of residues in this region and CIB1 binding affinity. Even though binding affinity increases as the total side chain hydrophobicity in this region decreases, the least hydrophobic peptide, αM, had the weakest binding affinity. This indicates that an optimal range of hydrophobicities of these residues coincides with a stronger binding affinity of CIB1. On the basis of this observed relationship, we calculated the hydrophobicities of the highly varied region of the consensus motif in all α-integrins. Because the test set includes representative members of each integrin subfamily and all of the calculated hydrophobicities fall within the range of the tested integrins, we conclude that the strength of binding of CIB1 to all α-integrins can be categorized as moderate if the highly varied region is hydrophobic or weak if this region is hydrophilic. These hydrophobicity data do not, however, explain why αIIb exhibits exothermic binding while the other peptides exhibit endothermic binding. We suspect that the Ala in position 4 (Ala^{1017}) of the αIIb peptide is necessary but not sufficient to cause this difference in enthalpy. This is evidenced in part by the Ala substitutions made in the αV peptides where the enthalpy of binding to CIB1 goes from endothermic with the WT peptide to exothermic with the 4-Ala peptide. We believe that this is not sufficient, however, because αM, which has an Ala in the same position, exhibits endothermic binding. Further testing is required to clarify how the integrin sequence affects the thermodynamic properties of binding to CIB1.

The new mechanistic details revealed by thermodynamc measurements of the CIB1-integrin interaction have provided some insight into the potential biological role of CIB1 in integrin function. We were surprised to find that the enthalpies of binding between CIB1 and the newly tested α-integrin sequences differed from that of αIIb, yet the binding affinities were relatively similar to one another. This may indicate that there is an αIIb-specific binding mechanism, which begs the

question of whether different binding mechanisms correlate with different functional roles. Previous evidence indicated that CIB1 plays a role in inside-out integrin signaling by negatively regulating αIIbβ3 activation in thrombin-stimulated megakaryocytes[19] and contributes to outside-in signaling by regulating cell spreading through focal adhesion kinase (FAK).[20,21] Whether CIB1 plays similar roles with other integrins, or different roles, as potentially implied by its distinct thermodynamic binding properties with other integrins, is currently unknown but will be of interest for future studies.

In conclusion, we present data that show that CIB1 binds to seven additional α-integrin CT peptides, bringing the total number of α-integrins that can associate with CIB1 to eight. Because some α-integrins may form heterodimers with multiple β-integrins (e.g., αVβ1 and αVβ3), we infer that the total number of integrin complexes with which CIB1 interacts is 13. On the basis of sequence comparisons of the cytoplasmic membrane-proximal regions of the 10 remaining α-integrin subunits, we predict that CIB1 could bind to all 24 known integrin heterodimers. These findings suggest that CIB1 may be a much broader regulator of integrin function than previously realized. Additionally, broad integrin binding activity is potentially conserved across CIB family proteins as indicated by the finding that CIB2 binds to α7 and αIIb.[45,46] Because this study suggests that CIB1 may act as a broad regulator of integrin function and recent evidence revealed that CIB1 plays a vital role in cancer cell survival,[47] it is important to further investigate mechanistic and functional details of CIB1−integrin interactions.

■ ASSOCIATED CONTENT

Supporting Information

Figures of an alignment of all α-integrin cytoplasmic tails and ITC titration isotherms and a table showing the sequences of all tested α-integrin CT peptides. This material is available free of charge via the Internet at http://pubs.acs.org.

■ AUTHOR INFORMATION

Corresponding Author

*Department of Biochemistry and Biophysics, 3016 Genetic Medicine CB#7260, 120 Mason Farm Rd., University of North Carolina at Chapel Hill, Chapel Hill, NC 27599-7260. E-mail: leslie_parise@med.unc.edu. Telephone: (919) 966-2238. Fax: (919) 966-2852.

Present Address

†Y.I.W.: UConn Health Center, Center for Cell Analysis and Modeling, Cell and Genome Sciences Building, MC 6406, 400 Farmington Ave., Farmington, CT 06030.

Author Contributions

T.M.L. and L.V.P. are co-senior authors.

Funding

This work was supported by National Institutes of Health Grants R01 HL092544 to L.V.P., R21 NS071216 to Y.I.W., and RO1 GM080742 to N.V.D., and T.C.F. was supported through the National Institute of General Medical Sciences IRACDA Program 5K12-GM000678. O.D. is a Howard Hughes Medical Institute International Student Research Fellow.

Notes

The authors declare no competing financial interest.

■ ACKNOWLEDGMENTS

Thanks to Feng Ding for assistance with computational modeling. We also thank Jun Qin of the Cleveland Clinic (Cleveland, OH) for many helpful discussions and early insights.

■ ABBREVIATIONS

BCA, bicinchoninic acid; CIB1, calcium and integrin binding protein 1; Co-IP, co-immunoprecipitation; CT, cytoplasmic tail; DMD, discrete molecular dynamics; ELISA, enzyme-linked immunosorbant assay; FAK, focal adhesion kinase; GAIP, Gα-interacting protein; GIPC1, GAIP C-terminal interacting protein 1; HEK293T, human embryonic kidney 293 temperature-sensitive cells; HEPES, 4-(2-hydroxyethyl)piperazine-1-ethanesulfonic acid; HB, hydrogen bonding; HI, hydrophobic interactions; ITC, isothermal titration calorimetry; LB, Luria-Bertani broth; MBP, maltose binding protein; PAK1, p21 activated kinase 1; PBS, phosphte-buffered saline; RH, regulator of G protein signaling homology; SDS−PAGE, sodium dodecyl sulfate−polyacrylamide gel electrophoresis; SHARPIN, shank-associated RH domain interactor; TEV, tobacco etch virus protease.

■ REFERENCES

(1) Hynes, R. O. (2002) Integrins: Bidirectional, allosteric signaling machines. *Cell 110*, 673−687.

(2) Felding-Habermann, B. (2003) Integrin adhesion receptors in tumor metastasis. *Clin. Exp. Metastasis 20*, 203−213.

(3) Kato, A. (1997) The biologic and clinical spectrum of Glanzmann's thrombasthenia: Implications of integrin αIIbβ3 for its pathogenesis. *Crit. Rev. Oncol. Hematol. 26*, 1−23.

(4) Yonekawa, K., and Harlan, J. M. (2005) Targeting leukocyte integrins in human diseases. *J. Leukocyte Biol. 77*, 129−140.

(5) Knezevic, I., Leisner, T. M., and Lam, S. C. (1996) Direct binding of the platelet integrin αIIbβ3 (GPIIb-IIIa) to talin. Evidence that interaction is mediated through the cytoplasmic domains of both αIIb and β3. *J. Biol. Chem. 271*, 16416−16421.

(6) Moser, M., Nieswandt, B., Ussar, S., Pozgajova, M., and Fassler, R. (2008) Kindlin-3 is essential for integrin activation and platelet aggregation. *Nat. Med. 14*, 325−330.

(7) Rantala, J. K., Pouwels, J., Pellinen, T., Veltel, S., Laasola, P., Mattila, E., Potter, C. S., Duffy, T., Sundberg, J. P., Kallioniemi, O., Askari, J. A., Humphries, M. J., Parsons, M., Salmi, M., and Ivaska, J. (2011) SHARPIN is an endogenous inhibitor of β1-integrin activation. *Nat. Cell Biol. 13*, 1315−1324.

(8) Mai, A., Veltel, S., Pellinen, T., Padzik, A., Coffey, E., Marjomaki, V., and Ivaska, J. (2011) Competitive binding of Rab21 and p120RasGAP to integrins regulates receptor traffic and migration. *J. Cell Biol. 194*, 291−306.

(9) Valdembri, D., Caswell, P. T., Anderson, K. I., Schwarz, J. P., Konig, I., Astanina, E., Caccavari, F., Norman, J. C., Humphries, M. J., Bussolino, F., and Serini, G. (2009) Neuropilin-1/GIPC1 signaling regulates α5β1 integrin traffic and function in endothelial cells. *PLoS Biol. 7*, e25.

(10) Alahari, S. K., and Nasrallah, H. (2004) A membrane proximal region of the integrin α5 subunit is important for its interaction with nischarin. *Biochem. J. 377*, 449−457.

(11) Coppolino, M., Leung-Hagesteijn, C., Dedhar, S., and Wilkins, J. (1995) Inducible interaction of integrin α2β1 with calreticulin. Dependence on the activation state of the integrin. *J. Biol. Chem. 270*, 23132−23138.

(12) Naik, U. P., Patel, P. M., and Parise, L. V. (1997) Identification of a novel calcium-binding protein that interacts with the integrin αIIb cytoplasmic domain. *J. Biol. Chem. 272*, 4651−4654.

(13) Shock, D. D., Naik, U. P., Brittain, J. E., Alahari, S. K., Sondek, J., and Parise, L. V. (1999) Calcium-dependent properties of CIB binding

to the integrin αIIb cytoplasmic domain and translocation to the platelet cytoskeleton. *Biochem. J. 342* (Part 3), 729−735.
(14) Gentry, H. R., Singer, A. U., Betts, L., Yang, C., Ferrara, J. D., Sondek, J., and Parise, L. V. (2005) Structural and biochemical characterization of CIB1 delineates a new family of EF-hand-containing proteins. *J. Biol. Chem. 280*, 8407−8415.
(15) Huang, H., and Vogel, H. J. (2012) Structural Basis for the Activation of Platelet Integrin αIIbβ3 by Calcium- and Integrin-Binding Protein 1. *J. Am. Chem. Soc. 134*, 3864−3872.
(16) Yamniuk, A. P., Anderson, K. L., Fraser, M. E., and Vogel, H. J. (2009) Auxiliary Ca^{2+} binding sites can influence the structure of CIB1. *Protein Sci. 18*, 1128−1134.
(17) Yamniuk, A. P., Nguyen, L. T., Hoang, T. T., and Vogel, H. J. (2004) Metal ion binding properties and conformational states of calcium- and integrin-binding protein. *Biochemistry 43*, 2558−2568.
(18) Barry, W. T., Boudignon-Proudhon, C., Shock, D. D., McFadden, A., Weiss, J. M., Sondek, J., and Parise, L. V. (2002) Molecular basis of CIB binding to the integrin αIIb cytoplasmic domain. *J. Biol. Chem. 277*, 28877−28883.
(19) Yuan, W., Leisner, T. M., McFadden, A. W., Wang, Z., Larson, M. K., Clark, S., Boudignon-Proudhon, C., Lam, S. C., and Parise, L. V. (2006) CIB1 is an endogenous inhibitor of agonist-induced integrin αIIbβ3 activation. *J. Cell Biol. 172*, 169−175.
(20) Naik, M. U., and Naik, U. P. (2003) Calcium-and integrin-binding protein regulates focal adhesion kinase activity during platelet spreading on immobilized fibrinogen. *Blood 102*, 3629−3636.
(21) Naik, U. P., and Naik, M. U. (2003) Association of CIB with GPIIb/IIIa during outside-in signaling is required for platelet spreading on fibrinogen. *Blood 102*, 1355−1362.
(22) Kauselmann, G., Weiler, M., Wulff, P., Jessberger, S., Konietzko, U., Scafidi, J., Staubli, U., Bereiter-Hahn, J., Strebhardt, K., and Kuhl, D. (1999) The polo-like protein kinases Fnk and Snk associate with a Ca^{2+}- and integrin-binding protein and are regulated dynamically with synaptic plasticity. *EMBO J. 18*, 5528−5539.
(23) Leisner, T. M., Liu, M., Jaffer, Z. M., Chernoff, J., and Parise, L. V. (2005) Essential role of CIB1 in regulating PAK1 activation and cell migration. *J. Cell Biol. 170*, 465−476.
(24) Yuan, W., Leisner, T. M., McFadden, A. W., Clark, S., Hiller, S., Maeda, N., O'Brien, D. A., and Parise, L. V. (2006) CIB1 is essential for mouse spermatogenesis. *Mol. Cell. Biol. 26*, 8507−8514.
(25) Denofrio, J. C., Yuan, W., Temple, B. R., Gentry, H. R., and Parise, L. V. (2008) Characterization of calcium- and integrin-binding protein 1 (CIB1) knockout platelets: Potential compensation by CIB family members. *Thromb. Haemostasis 100*, 847−856.
(26) Heineke, J., Auger-Messier, M., Correll, R. N., Xu, J., Benard, M. J., Yuan, W., Drexler, H., Parise, L. V., and Molkentin, J. D. (2010) CIB1 is a regulator of pathological cardiac hypertrophy. *Nat. Med. 16*, 872−879.
(27) Zayed, M. A., Yuan, W., Chalothorn, D., Faber, J. E., and Parise, L. V. (2010) Tumor growth and angiogenesis is impaired in CIB1 knockout mice. *J. Angiog. Res. 2*, 17.
(28) Zayed, M. A., Yuan, W., Leisner, T. M., Chalothorn, D., McFadden, A. W., Schaller, M. D., Hartnett, M. E., Faber, J. E., and Parise, L. V. (2007) CIB1 regulates endothelial cells and ischemia-induced pathological and adaptive angiogenesis. *Circ. Res. 101*, 1185−1193.
(29) Hwang, P. M., and Vogel, H. J. (2000) Structures of the platelet calcium- and integrin-binding protein and the αIIb-integrin cytoplasmic domain suggest a mechanism for calcium-regulated recognition; homology modelling and NMR studies. *J. Mol. Recognit. 13*, 83−92.
(30) Roy, A., Kucukural, A., and Zhang, Y. (2010) I-TASSER: A unified platform for automated protein structure and function prediction. *Nat. Protoc. 5*, 725−738.
(31) Yang, J., Ma, Y. Q., Page, R. C., Misra, S., Plow, E. F., and Qin, J. (2009) Structure of an integrin αIIbβ3 transmembrane-cytoplasmic heterocomplex provides insight into integrin activation. *Proc. Natl. Acad. Sci. U.S.A. 106*, 17729−17734.
(32) *The PyMOL Molecular Graphics System*, version 1.4.1 (2010) Schrodinger, LLC, Portland, OR.
(33) Dagliyan, O., Proctor, E. A., D'Auria, K. M., Ding, F., and Dokholyan, N. V. (2011) Structural and dynamic determinants of protein-peptide recognition. *Structure 19*, 1837−1845.
(34) Yin, S., Biedermannova, L., Vondrasek, J., and Dokholyan, N. V. (2008) MedusaScore: An accurate force field-based scoring function for virtual drug screening. *J. Chem. Inf. Model. 48*, 1656−1662.
(35) Ding, F., Yin, S., and Dokholyan, N. V. (2010) Rapid flexible docking using a stochastic rotamer library of ligands. *J. Chem. Inf. Model. 50*, 1623−1632.
(36) Yamniuk, A. P., Ishida, H., and Vogel, H. J. (2006) The interaction between calcium- and integrin-binding protein 1 and the αIIb integrin cytoplasmic domain involves a novel C-terminal displacement mechanism. *J. Biol. Chem. 281*, 26455−26464.
(37) Huang, H., Ishida, H., Yamniuk, A. P., and Vogel, H. J. (2011) Solution structures of Ca^{2+}-CIB1 and Mg^{2+}-CIB1 and their interactions with the platelet integrin αIIb cytoplasmic domain. *J. Biol. Chem. 286*, 17181−17192.
(38) Haas, T. A., Taherian, A., Berry, T., and Ma, X. (2008) Identification of residues of functional importance within the central turn motifs present in the cytoplasmic tails of integrin αIIb and αV subunits. *Thromb. Res. 122*, 507−516.
(39) Vallar, L., Melchior, C., Plancon, S., Drobecq, H., Lippens, G., Regnault, V., and Kieffer, N. (1999) Divalent cations differentially regulate integrin αIIb cytoplasmic tail binding to β3 and to calcium- and integrin-binding protein. *J. Biol. Chem. 274*, 17257−17266.
(40) Yamniuk, A. P., and Vogel, H. J. (2005) Calcium- and magnesium-dependent interactions between calcium- and integrin-binding protein and the integrin αIIb cytoplasmic domain. *Protein Sci. 14*, 1429−1437.
(41) Holdgate, G. A. (2007) Thermodynamics of binding interactions in the rational drug design process. *Expert Opin. Drug Discovery 2*, 1103−1114.
(42) Wimley, W. C., and White, S. H. (1996) Experimentally determined hydrophobicity scale for proteins at membrane interfaces. *Nat. Struct. Biol. 3*, 842−848.
(43) Proctor, E. A., Yin, S., Tropsha, A., and Dokholyan, N. V. (2012) Discrete molecular dynamics distinguishes nativelike binding poses from decoys in difficult targets. *Biophys. J. 102*, 144−151.
(44) Yamniuk, A. P., Gifford, J. L., Linse, S., and Vogel, H. J. (2008) Effects of metal-binding loop mutations on ligand binding to calcium- and integrin-binding protein 1. Evolution of the EF-hand? *Biochemistry 47*, 1696−1707.
(45) Huang, H., Bogstie, J. N., and Vogel, H. J. (2012) Biophysical and structural studies of the human calcium- and integrin-binding protein family: Understanding their functional similarities and differences. *Biochem. Cell Biol. 90*, 646−656.
(46) Hager, M., Bigotti, M. G., Meszaros, R., Carmignac, V., Holmberg, J., Allamand, V., Akerlund, M., Kalamajski, S., Brancaccio, A., Mayer, U., and Durbeej, M. (2008) Cib2 binds integrin α7Bβ1D and is reduced in laminin α2 chain-deficient muscular dystrophy. *J. Biol. Chem. 283*, 24760−24769.
(47) Leisner, T. M., Moran, C., Holly, S. P., and Parise, L. V. (2013) CIB1 prevents nuclear GAPDH accumulation and non-apoptotic tumor cell death via AKT and ERK signaling. *Oncogene 32*, 4017−4027.